

Percolation: Statistical Description of a Spatial and Temporal Highly Resolved Boundary Layer Transition

Tom T. B. Wester, Dominik Traphan, Gerd Gülker and Joachim Peinke

Abstract In this article spatio-temporally resolved particle image velocimetry data of a flat plate's boundary layer are shown. With this set up, it is possible to capture the highly unsteady phase transition from laminar to turbulent state of the boundary layer close to the surface. In the evaluation of the boundary layer data it is shown that it is possible to link the laminar-turbulent phase transition to the (2+1)D directed percolation universality class. This can be shown by the unique exponents of the directed percolation class which will be extracted from the PIV data.

1 Introduction

The description of transition into turbulence has always been a challenging task. Thirty years ago Pomeau was the first to describe the dynamics of laminar-turbulent transition by a system of coupled oscillators [1]. Thereby he paved the way for the statistical description of laminar-turbulent transition by the directed percolation theory. This theory allows a simple description of complex phase transitions with only three critical exponents. These exponents are unique for each universality class of percolation, so the transition from a laminar to a turbulent flat plate's boundary layer may be ascribed to a known class.

Until the last decade it was not possible to provide experimental evidence to show the spatio-temporal intermittency which occurs in the transition from laminar to turbulent flow. Due to more accurate measurement techniques nowadays it is possible to capture the transition with much higher temporal and spatial resolution.

This has led to more detailed investigations with respect to directed percolation of different flow situations such as channel flow [2, 3], Couette flow [4], shear flows [5–8] and fully turbulent flows [9]. All of them show promising results, which support the presumption of Pomeau.

T.T.B. Wester (✉) · D. Traphan · G. Gülker · J. Peinke
ForWind, Institute of Physics, University of Oldenburg, Oldenburg, Germany
e-mail: tom.wester@uol.de

In contrast to the experiments mentioned, the evaluation presented in this article is the first which is carried out on a flat plate's boundary layer in an airflow and also the first evaluation which uses PIV data as basis.

2 Experimental Setup and Methodology

The experiment is based on high speed stereoscopic particle image velocimetry (HS-PIV). In order to investigate the boundary layer of the flat plate, a wind tunnel with a closed test section is used (see Fig. 1). It has a cross section of $25 \times 25 \text{ cm}^2$ and a length of 200 cm. The flat plate under investigation has a length of 100 cm. It is positioned 30 cm downstream the wind tunnel nozzle at a height of 10 cm above the bottom of the test section.

The experiment is performed at a velocity of $u_\infty = 11.5 \text{ m s}^{-1}$ and a free stream turbulence intensity below 0.3%. Due to the limited field of view (FOV) of the PIV measurements it is necessary to induce perturbations into the boundary layer. Therefore a small step of 0.1 mm height is placed 5 cm downstream the leading edge. Hereby the transition area can be tuned so that its streamwise length fits into the HS-PIV FOV.

The used HS-PIV system consisted of a high speed laser LDY 303 by Litron, light sheet optics and two Phantom Miro M320S high-speed cameras which are used at a reduced resolution of $1408 \times 1048 \text{ px}^2$ resulting in 154×126 PIV interrogation windows. The light sheet is directed perpendicular to the inflow direction and illuminates a plane parallel to the plate's surface. The origin of the plane is located 5.8 cm downstream of the leading edge. In focus the light sheet has a thickness of 1 mm and

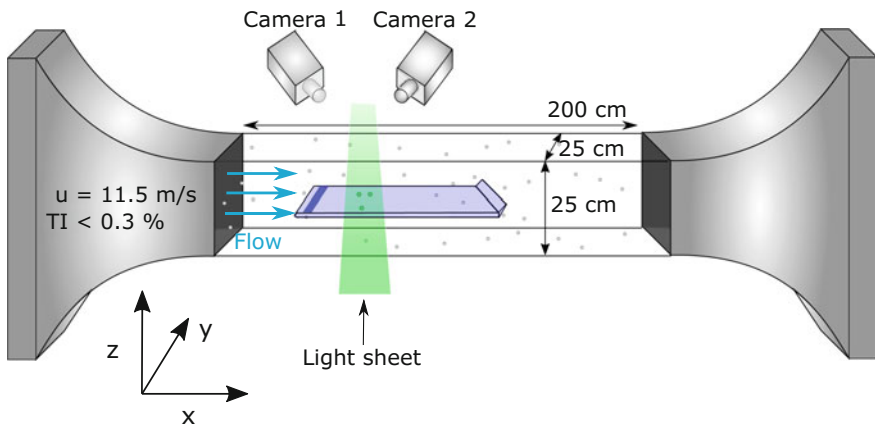


Fig. 1 Experimental setup for HSPIV measurements of a flat plate's boundary layer. The light sheet is adjusted parallel to the flat plate's surface in a region where the onset of the transition can be captured

its height above the plate's surface is 1 mm. The boundary layer thickness estimated by the Blasius equation is 2 mm at the point of measurement. Thus, the upper half of the boundary layer is investigated in the PIV measurement.

With this set up a sampling rate of 1000 velocity fields per second is possible. The velocity fields have a size of 6 cm in streamwise (x -direction) and 5 cm in spanwise direction (y -direction) with a spatial resolution of 0.04 cm in each direction. In total, 8250 velocity fields in three independent measurements are acquired. Each measurement has a duration of 2.75 s, because of the limited internal camera storage. Particle images are captured and processed using LaVision software DaVis 8.3.

3 Experimental Data

In the percolation theory only two states exist: a cell is either laminar (off) or turbulent (on). For this reason, all velocity fields need to be binarized by a certain criterion. In Fig. 2a snapshot of the velocity magnitude is plotted. Shown is the development of the velocity along the local Reynolds number $Re_x = \frac{u(x) \cdot x}{\nu}$ where x is the denoted as the propagation length along the plate and the spanwise direction. The right hand side shows the same velocity field, but binarized.

In order to binarize the data, a velocity threshold is used. Based on the velocity, one can directly draw a conclusion on the state of the boundary layer. If the velocity increases compared to the laminar boundary layer there must be a mixing between the high energetic ambient flow and the low energetic boundary layer. This only happens if the boundary layer becomes unstable and thus transitive and turbulent.

According to that, the interrogation cell is set to 0 (off) if $u(x)_{TH}$ and 1 (on) otherwise. A parameter variation yielded $u_{TH} = 4 \text{ m s}^{-1}$ as an appropriate threshold that reflects turbulent structures for the given measurement distance to the wall. However, percolation exponents do only slightly depend on chosen velocity threshold.

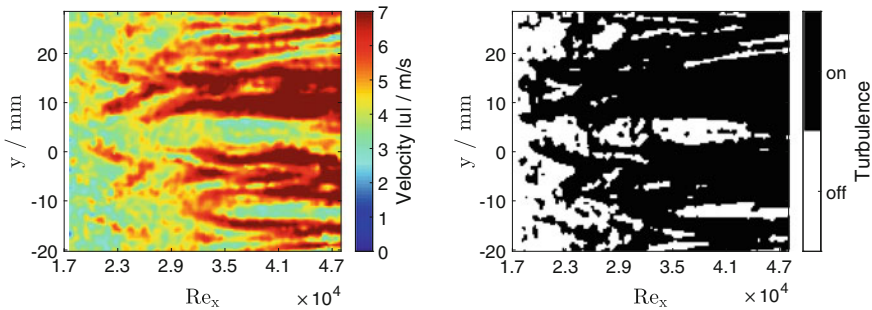


Fig. 2 *Left* Example of a measured velocity field. *Right* Binarized velocity field by a threshold of $u_{Thresh} = 4 \text{ ms}^{-1}$

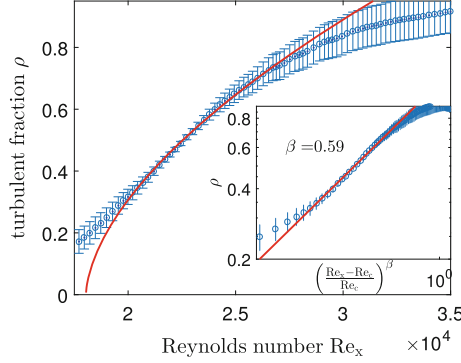


Fig. 3 Scaling of turbulent fraction with Reynolds number $Re_x = \frac{u(x) \cdot x}{\nu}$ in streamwise direction. The measurement points are shown in *blue* with *error bars*. The *red curve* represents a fit according to (1). The *inset* shows the plot in logarithmic scale to emphasize the exponential behavior. Here, the turbulent fraction is plotted against the reduced Reynolds number

The turbulent fraction $\rho(Re_x)$ can be determined directly from the binarized data. The turbulent fraction is the ratio of turbulent to laminar cells for each interrogation window. For this reason, a two-dimensional turbulent fraction results for the PIV data. This two-dimensional turbulent fraction is averaged along the y -direction to obtain a one-dimensional distribution. This distribution is plotted against the local Reynolds number Re_x in Fig. 3. The shown errorbars represent the standard deviation. The inset of the figure shows the logarithmic illustration of the turbulent fraction over the reduced Reynolds number $\frac{Re_x - Re_c}{Re_c}$. The turbulent fraction shows a monotonic growth with increasing local Reynolds number. At the so called critical point the turbulent fraction increases rapidly. This is typical for directed percolation and can be described by the exponential relation between the turbulent fraction $\rho(Re_x)$, the local Reynolds number Re_x and the critical point Re_c shown in (1):

$$\rho(Re_x) = \rho_0 \cdot \left(\frac{Re_x - Re_c}{Re_c} \right)^\beta. \quad (1)$$

In this equation ρ_0 is a constant factor and the exponent β is one of three unique exponents of percolation theory which describes the increase of the turbulent fraction.

In percolation theory, Re_c is the point where the phase transition between two states happens. In our case, it is the point where the transition between laminar and turbulent phase begins. In case of the experiment, this corresponds to the point at which the turbulent fraction begins to grow strongly.

The fit with (1) results in a critical Reynolds number $Re_c = 18040 \pm 380$ and the exponent $\beta_{exp} = 0.59 \pm 0.04$. In order to obtain the other two unique exponents of percolation theory μ_{\parallel} and μ_{\perp} which describe the spatial and temporal spreading behavior, the development of laminar clusters must be considered. Laminar cluster are regions in the time development of the flow at Re_c where laminar cells are

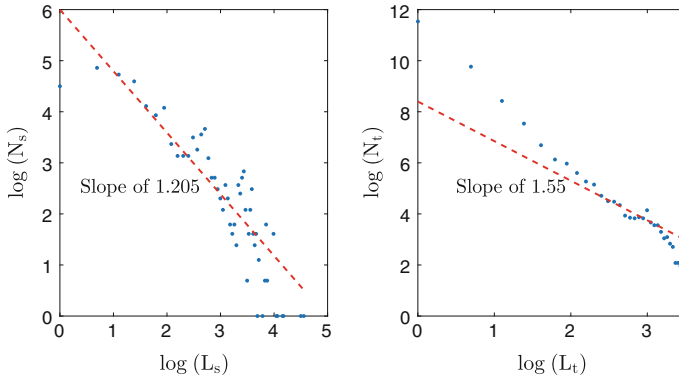


Fig. 4 *Left* Histogram of laminar clusters in space. *Red dashed line* represents the theoretical slope of (2+1)D directed percolation. *Right* Histogram of laminar clusters in time. *Red dashed line* represents the theoretical slope of (2+1)D directed percolation

surrounded by turbulent cells. In percolation theory, the number ($N_{s,t}$) of clusters of a particular size ($L_{s,t}$) scale with the following laws for space (2) and time (3):

$$N_s(L_s) \propto L_s^{\mu_\perp} \quad (2)$$

$$N_t(L_t) \propto L_t^{\mu_\parallel}. \quad (3)$$

The histograms of the cluster sizes are shown in Fig. 4. On the left hand side, the laminar cluster sizes in space, and on the right hand side, the cluster sizes in time are shown. The red dashed lines show slopes of the theoretical cluster distribution in (2+1)D directed percolation theory.

4 Discussion and Concluding Remarks

In the preceding chapter, the experimental results were presented. From the turbulent fraction, the first unique exponent β is derived. This exponent is close to the theoretical exponent for (2+1)D directed percolation $\beta_{theo} = 0.583$. The other unique exponents for the scaling behavior of the cluster sizes also follow the laws of (2+1)D directed percolation visually. The cluster in space follow the law better than the clusters in time. The small deviation could be a result of the limited temporal resolution. Another explanation is a limited size effect due to the limited FOV of the PIV measurements.

All in all, the transition of the flat plate's boundary layer can be described by the (2+1)D directed percolation theory. The extracted exponents from the experiment seem to match the theory. Therefore, the highly dynamic behavior of the transition can be reduced to mainly three unique exponents and this phenomenon can be assigned to one of the known percolation classes.

5 Future Work

Since these first results are promising a validation is needed. Therefore, the turbulent boundary layer of the flat plate will be investigated more detailed at different heights and at different free stream velocities.

Furthermore, other transient flows such as channel flow or even more complex flows such as airfoil boundary layers will be investigated. If it is possible to show that transitions from laminar to turbulent flow belong to a universality class of percolation this results could be used for computational fluid dynamic models to simulate the transition in a more accurate way.

Acknowledgements The authors thank the Niedersächsische Ministerium für Wissenschaft und Kultur (Ministry of Science and Culture of Lower Saxony) for financial support.

References

1. Y. Pomeau, Front motion, metastability and subcritical bifurcations in hydrodynamics. *Physica D: Nonlinear Phenomena* **23**(1), 3–11 (1986)
2. D. Barkley, Simplifying the complexity of pipe flow. *Physical Review E* **84**(1), 016309 (2011)
3. M. Sano, K. Tamai, A universal transition to turbulence in channel flow. *Nature Physics*, 2016
4. G. Lemoult, L. Shi, K. Avila, S.V Jalikop, M. Avila, B. Hof, Directed percolation phase transition to sustained turbulence in couette flow. *Nature Physics*, 2016
5. T. Korinna, Allhoff and Bruno Eckhardt. Directed percolation model for turbulence transition in shear flows. *Fluid Dynamics Research* **44**(3), 031201 (2012)
6. T. Kreilos, B. Eckhardt, T.M Schneider. Increasing lifetimes and the growing saddles of shear flow turbulence. *Physical review letters*, **112**(4):044503, 2014
7. H.-Y. Shih, T.-L. Hsieh, N. Goldenfeld. Ecological collapse and the emergence of travelling waves at the onset of shear turbulence. *Nature Physics*, 2015
8. M. Avila, B. Hof, Nature of laminar-turbulence intermittency in shear flows. *Physical Review E* **87**(6), 063012 (2013)
9. D. Barkley, B. Song, V. Mukund, G. Lemoult, M. Avila, B. Hof, The rise of fully turbulent flow. *Nature* **526**(7574), 550–553 (2015)

Progress in Turbulence VII

Proceedings of the iTi Conference in Turbulence 2016

Örlü, R.; Talamelli, A.; Oberlack, M.; Peinke, J. (Eds.)

2017, XV, 250 p. 113 illus., 89 illus. in color., Hardcover

ISBN: 978-3-319-57933-7